

One-dimensional turbulence (ODT): computationally efficient modeling and simulation of turbulent flows

Victoria B. Stephens, David O. Lignell*

Chemical Engineering Department, Brigham Young University, Provo, UT 84602, USA

Abstract

Write this last. About 100 words.

Keywords: turbulence, reacting flows, one-dimensional turbulence

Code Metadata

Nr.	Code metadata description	Please fill in this column
C1	Current code version	1.0
C2	Permanent link to code/repository used for this code version	<i>github.com/BYUignite/ODT</i>
C3	Code Ocean compute capsule	N/A
C4	Legal Code License	MIT
C5	Code versioning system used	Git
C6	Software code languages, tools, and services used	C++, Python 3.x, Yaml,
C7	Compilation requirements, operating environments & dependencies	CMake 3.12+, Cantera, Git, Doxygen (optional)
C8	If available Link to developer documentation/manual	N/A
C9	Support email for questions	davidlignellbyu.edu

Table 1: Code metadata (mandatory)

1. Motivation and significance

Turbulent flows characterize the vast majority of fluid flows in practical engineering applications, and simulations of turbulent flows provide re-

*Corresponding author.

Email address: davidlignell@byu.edu (David O. Lignell)

4 searchers with valuable insights into complex systems, particularly reacting
5 turbulent flows such as combustion processes. Turbulence is a complex phe-
6 nomenon that affects the full range of a flow’s length and time scales. As a
7 result, resolving the entire flow field by numerically solving the Navier-Stokes
8 equations of fluid flow, as is done in direct numerical simulations (DNS), re-
9 quires substantial computational resources. DNS is a powerful research tool,
10 but its high computational cost makes it intractable for simulating most
11 practical engineering flows. In order to achieve numerical solutions to prac-
12 tical flow problems, researchers can use alternative frameworks that model
13 turbulence rather than resolving it directly.

14 Large-eddy simulations (LES) address the problem of wide-ranging length
15 and time scales by combining direct resolution of grid-scale quantities, as in
16 DNS, with subgrid modeling of smaller turbulence structures. The more
17 complex the flow, the more modeling is required; for example, a jet flame
18 simulation might require subgrid modeling for the combustion chemistry, ra-
19 diative heat transfer, or soot chemistry in addition to turbulence structures,
20 all of which form a tightly coupled system in which each model interacts
21 heavily with the others. While subgrid modeling makes LES more computa-
22 tionally affordable than DNS, it can introduce empiricism into simulations,
23 which can lead to inaccurate results. Additionally, unresolved quantities are
24 often parameterized in state space with empirical relationships or assumed
25 distributions that lack universal applicability. LES is a valuable simulation
26 tool, but its approach to turbulence modeling can introduce unwanted em-
27 piricism and make errors difficult to isolate and quantify.

28 The one-dimensional turbulence model (ODT) functionally reverses the
29 LES approach, modeling large-scale turbulent advection and directly resolv-
30 ing small-scale flow structures, simulating the full range of length and time
31 scales in a single dimension. Because large-scale structures are much easier
32 to study and model than small-scale structures, ODT mitigates or sidesteps
33 many of the subgrid modeling issues that complicate LES. Previous stud-
34 ies show that ODT can attain accuracy comparable to DNS at a fraction
35 of the computational cost [1, 2], making it an attractive tool for simulating
36 turbulent flows. Because the ODT model is one-dimensional, it is limited to
37 homogeneous or boundary-layer flows, such as jets, wakes, and mixing layers;
38 these types of flows, however, are common in nature and central to turbu-
39 lence research. ODT’s computational efficiency and resolution of a full range
40 of scales make it a valuable tool that complements experimental studies and
41 other simulation tools like DNS and LES.

42 Early applications of ODT focused on homogenous turbulence, wakes, and
43 mixing layers [3, 4, 5]. Later extension to variable-density flows and a spatial
44 downstream coordinate system facilitated its growth and application to more

complex flows, including combustion in jet flames [6, 7, 8, 9, 10, 11, 12, 13], counterflow flames [14], wall fires [15], and sooting flames [1, 16, 17, 18, 19], as well as other particle flows [20, 21, 22, 23]. ODT has also served to complement LES through subgrid modeling studies [24, 25, 26] and has been applied to various other flow configurations such as double-diffusive interfaces [27], Rayleigh-Taylor mixing [28], and stratified turbulence [29]. Most recently, the ODT code was extended to include cylindrical and spherical coordinate systems [30, 31, 32].

During the recent implementation of the cylindrical and spherical model formulations, the ODT code was drastically overhauled and reorganized, resulting in its current configuration. The ODT code presented here is a pared down version of the development code, representing the fundamental aspects of the ODT model and its most reliable functions. The example cases in Section 3 are a representative sample of the ODT code’s capabilities as it is presented here. Future releases will expand this code’s functionality with additional features currently in development.

2. Software description

2.1. Model description

The ODT model is described in detail in the literature [3, 5, 33, 30, 34]; only a brief explanation will be given here. In ODT, turbulent advection is modeled with stochastic processes called eddy events, which punctuate the solution of unsteady, one-dimensional transport equations for mass, momentum, and enthalpy. The ODT code uses a Lagrangian finite-volume formulation for diffusive advancement in which mass stays constant within each grid cell while cell volumes increase or decrease according to cell dilation via an adaptive mesh refinement [34].

Transport equations for mass, momentum, and enthalpy in the temporal formulation of ODT take the following generic form, derived from the Reynolds Transport Theorem [35] for a given scalar quantity per unit mass β :

$$\frac{d\beta}{dt} = -\frac{j_{\beta,e}A_{x,e} - j_{\beta,w}A_{x,w}}{\rho V} + \frac{S_{\beta}}{\rho V}. \quad (1)$$

Here, j_{β} is the diffusion flux of scalar β across the cell face area A_x where the subscripts e and w refer to the "east" and "west" faces of the grid cell, respectively. S_{β} is the Lagrangian source term derived from the conservation law for β , ρ represents mass density, and V represents cell volume. In practice, we refer to the left hand term on the right side of Equation 1 as the "mixing term" and the right hand term on the right side of Equation 1 as the "source term". The generic transport equation differs slightly in the spatial

formulation of ODT, but its form is the same, so we omit it here for brevity. The system of ordinary differential equations (ODEs) that results is well behaved at all grid points and in all geometries in their finite-volume forms. For details on transport equation derivation and use in both the temporal and spatial formulations of ODT, see Lignell et al. [30].

Eddy events occur as a Poisson process in accordance with their eddy rates, where a given eddy event of size l and location x_0 has an eddy timescale t and an associated eddy rate $1/t$. Three user-defined ODT parameters control the eddy event process: the eddy rate parameter C scales the rate of occurrence of the eddies; the viscous penalty parameter Z suppresses small eddies; and the large eddy suppression parameter β constrains eddies such that they do not reach over the elapsed simulation time. Sampled eddies that do not fit the defined parameters are rejected and not applied to the domain.

Eddy events modify domain variables using triplet maps, as illustrated for a cylindrical domain in Figure 1. For a region of eddy size l , the domain is copied to create three map images; the three images are then placed back to back with the middle image inverted to maintain continuity, and the composite is reapplied to the domain. This process applies to all transported variables on the domain. Applied properly, the triplet map increases scalar gradients and decreases length scales consistent with the application of turbulent eddies in real flows, conserves all quantities and their statistical moments, and maintains continuity in property profiles. Subsequent eddies in the same region will result in a cascade of scales, and eddy rates depend on eddy size and the local kinetic energy such that they follow turbulent cascade scaling laws.

Eddy events occur concurrently with diffusive advancement via solution of the system of unsteady one-dimensional transport equations. In this way, the ODT code marches in time or space until it reaches its end point. Due to the stochastic nature of eddy events, each ODT simulation, or realization, is different, even when it is provided with the same input parameters. In order to obtain statistically stable data for a given set of parameters, we run many realizations with the same input parameters and time-average them. This is done via post-processing tools, which are provided in the ODT package.

2.2. Software Architecture

The ODT package consists primarily of an object-oriented C++ code responsible for running flow simulation cases and generating data. The package also contains auxiliary data processing and visualization tools, written mostly in Python. The post-processing tools are case-specific but will be addressed in Section 2.3.

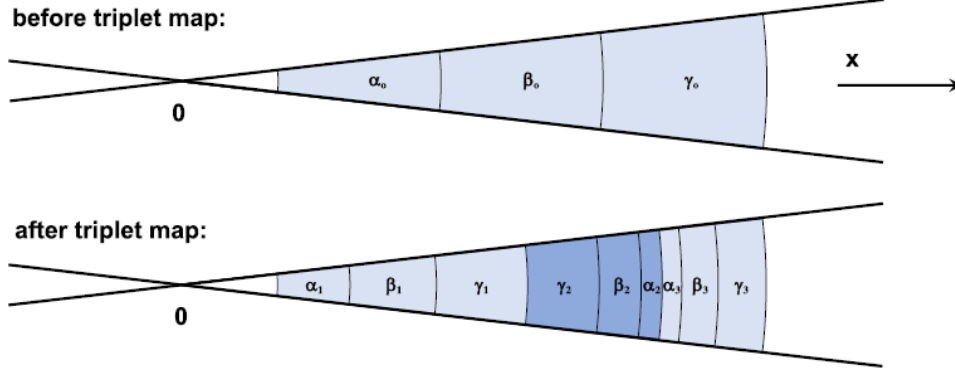


Figure 1: Schematic diagram of a cylindrical triplet map, adapted from [30]. Before the triplet map, the domain contains three grid cells of equal volume, while after the triplet map has been applied, the domain contains nine cells. The nine final cells are labeled according to the cells from which they originated and shaded to indicate that three map images were combined to create the final composite.

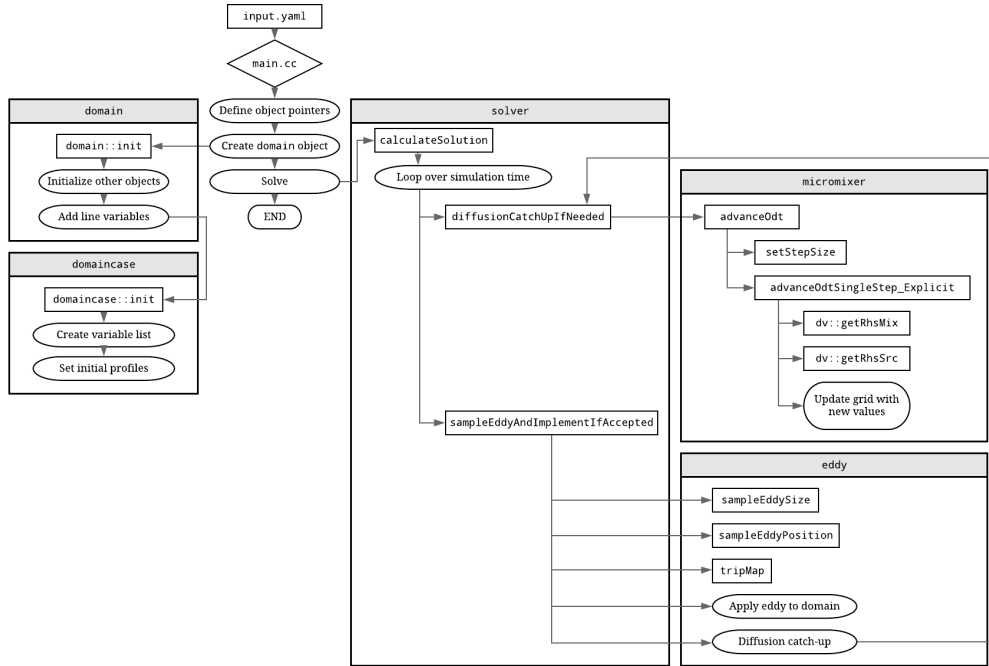


Figure 2: Basic structure of the ODT code. For clarity and brevity, this diagram makes two major assumptions: first, that diffusion advancement in the `micromixer` uses an explicit solution method; and second, that the eddy event sampled by the `eddy` object passes all rejection tests before being applied to the domain.

Figure 2 illustrates the ODT code’s most important objects and structural features. User inputs are provided to the executable in YAML [36] format via `input.yaml`; the location of the specific `input.yaml` file to be used is determined by the case name and case type specified in the run script. The `main` function defines storage for the main objects, but, once created, the `domain` object is responsible for object initialization as well as variable initialization and storage via a case-specific `domaincase` object.

Three primary objects handle the code’s main functions: the `solver`, `micromixer`, and `eddy` objects. The `solver` coordinates the ODT solution process, marching along the simulation time and invoking diffusive advancement and eddy events when appropriate. The `micromixer` handles diffusive advancement by setting step sizes, interacting with the transported domain variables, and solving the system of ODEs defined by Equation 1 (or its equivalent in the spatial formulation). The `micromixer` includes three solution methods that can be specified in `input.yaml`, each appropriate for various case types: a first-order explicit Euler method (pictured in Figure 2); a first-order semi-implicit method that uses CVODE [37] to advance coupled ODEs in individual grid cells, integrated sequentially; and a second-order Strang splitting method [38] good for treating stiff chemistry. In reacting flow cases, chemical kinetics are handled by Cantera [39], which uses transported variable values—enthalpy and gas species composition, for instance—to specify local scalar values such as gas temperature or density, which can affect flow properties. The `micromixer` is also the code’s primary point of interaction with the `mesher` object (not pictured in Figure 2), which manages the adaptive grid functions. Finally, the `eddy` object manages eddy event selection and implementation, which proceeds as described in Section 2.1.

2.3. Workflow

This section outlines the process a user would go through in order to successfully build the ODT code and run a simulation. For more details, please see the package documentation. ODT is a standalone, self-contained package, and users interact with its files primarily via the command line rather than a graphical interface.

Within the main download package, several directories organize the ODT package. The `source`, `build`, and `run` directories contain the ODT source code, compilation tools, and run scripts, respectively. The `input` directory contains subdirectories corresponding to several possible case types, each populated with an appropriate input files. The `data` directory, initially empty, holds the raw data files and runtime information generated by ODT, as well as post-processed data files generated from within the `post` directory.

161 Finally, the `doc` directory contains documentation optionally generated by
162 Doxygen [40] during the build process.

163 2.3.1. *Building ODT*

164 The ODT build process is relatively automated through CMake. First,
165 navigate to the `build` directory and edit the CMake configuration file. Note
166 that the user must specify which chemical mechanism to compile with before
167 building the code. In order to run simulations with different chemical mecha-
168 nisms, the code must be recompiled, including the CMake configuration files,
169 between simulations, whereas this is not required when other variables are
170 changed. This is a known inconsistency that will be changed in future code
171 releases. The CMake configuration file also specifies Cantera's location and
172 must be changed to reflect the local installation location. Once the settings
173 are correct, the user runs CMake to apply these changes.

174 YAML is required in order to process input files. If it has not yet been
175 installed, it is built and installed at this point. For convenience, the ODT
176 package includes the appropriate files and automates this process. YAML
177 need only be installed once for a given instance of the ODT package. Re-
178 building the ODT code with CMake does not affect the YAML installation.

179 Once CMake and YAML have been prepared, the user can build the ODT
180 code with the appropriate `make` command. There is no associated `install`
181 command that needs to be run. The most common errors that occur during
182 the build process concern incorrect file paths or incomplete installation of
183 precursor packages. See the build documentation for troubleshooting help.

184 Once the code is built, the user may optionally build a local copy of the
185 documentation via Doxygen, which must be previously installed. This step is
186 not required in order to run the ODT code. As an alternative, documentation
187 can be accessed via `README` files within the code or at the code repository
188 wiki.

189 2.3.2. *Input files*

190 User-modified input files are located within the `input` directory, which
191 contains subdirectories that correspond to various case types that can be run
192 with ODT. At minimum, a case's subdirectory contains an `input.yaml` file,
193 but may contain other files or subfolders. ODT has the capability to restart
194 a simulation from a specified time or state. To use this function, a raw data
195 file at the required state must be copied to the input case directory and
196 renamed `restart.dat`. For an example, please see the `jetFlame/flameD`
197 case. Note that the user must also change the `Lrestart` parameter within
198 the `input.yaml` file in order to use the restart feature. Input case directories
199 may also contain subdirectories with supplemental information or input file

Section	Description
params*	General parameters, including simulation length, domain size, and ODT parameters (C , Z , β_{LES})
radParams	Radiation parameters; only relevant to reacting flow cases (i.e. jet flames)
streamProps	Stream properties; used when there are two or more separate streams (i.e. non-premixed jets)
bcCond*	Boundary conditions for velocity and temperature (where required)
initParams	Case-specific initialization parameters, usually flow geometry and stream velocities
dumpTimes*	List of simulation time steps at which to output data files

Table 2: Common sections present in `input.yaml` files. Sections marked with a * should be present in every `input.yaml` file regardless of case type. Sections usually appear in this order, but this is not required.

examples; only the `input.yaml` file located in the base case input directory is used in a simulation.

The `input` directory also contains the `gas_mechanisms` subdirectory, which contains chemical mechanism files in XML format that can be used in reacting flow cases. For cases in which a chemical mechanism is not required, the `not_used.xml` mechanism file is specified in the appropriate `input.yaml` file in place of other mechanisms. Note that the chemical mechanism chosen for the case and specified in the input file must match the mechanism specified in the Cmake configuration file during the ODT build process.

Input files contain simulation parameters in a human-readable format parsed by YAML. Not all of the parameters in an input file may be used in a given simulation. An overview of possible ODT parameters will be covered here, but does not represent all the possibilities or functions of ODT; please see the associated documentation for more information. Input files are divided into sections, several of which are common to all `input.yaml` files; these are summarized in Table 2. Details about individual parameters, including usage and typical values, are covered in the documentation.

Prior to running a simulation, the user must select and modify the appropriate `input.yaml` file to reflect the desired conditions. The default values already present in the input files represent general parameters that may be used to run a successful simulation of that case type.

2.3.3. Running ODT

DETAILS GO HERE

223 3. Example Cases

224 3.1. Pipe Flow

225 First, we present an incompressible pipe flow simulation using the tempo-
226 ral, cylindrical ODT formulation. Results for three different friction Reynolds
227 numbers ($Re_\tau = 550, 1000, 2000$) are compared to DNS results from El
228 Khoury et al. [41] ($Re_\tau = 550, 1000$) and Chin et al. [42] ($Re_\tau = 2000$) for a
229 pipe diameter of $D = 2.0$ m and flow density of $1.0 \text{ kg}\cdot\text{m}^{-3}$. Friction velocity
230 values of $1 \text{ m}\cdot\text{s}^{-1}$ ($Re_\tau = 550, 1000$) and $2 \text{ m}\cdot\text{s}^{-1}$ ($Re_\tau = 2000$) were assumed
231 and used to calculate the mean pressure gradient driving the flow. Using
232 initial conditions with uniform velocity profiles, simulations were run until a
233 state of developed flow was achieved, at which point data were gathered until
234 statistical convergence for the root mean square (RMS) velocity difference
235 from the mean profiles occurred.

236 The simulations were performed with ODT parameters $C = 5$ and $Z =$
237 350 for the temporal ODT formulation. The values of C and Z were adjusted
238 to give good agreement of the ODT results compared to the DNS. Schmidt
239 et al. [25] showed that higher Z results in the buffer-layer being located
240 further from the wall, and increasing C results in a lower slope of the mean
241 streamwise velocity in the log-layer.

242 RESULTS AND PLOTS GO HERE

243 3.2. Non-reacting Jet

244 Here, we present ODT simulation results for a non-reacting round, tur-
245 bulent jet compared to the experimental data of Hussein et al. [43]. The
246 jet consists of air issuing into air through a 1 in (0.0254 m) diameter duct
247 with a uniform exit velocity of $56.2 \text{ m}\cdot\text{s}^{-1}$ and a reported Reynolds num-
248 ber of 95,500. The ODT simulations use this diameter and velocity with a
249 kinematic viscosity of $1.534 \cdot 10^{-5} \text{ m}^2\text{s}^{-1}$, resulting in a Reynolds number
250 of 93,056. The initial velocity profile in the ODT simulations is a modified
251 top-hat profile in which a hyperbolic tangent function of width $\delta = 0.1D$ is
252 used on either side of the jet to smooth the transition between the jet and
253 the free stream. In the spatial formulation of ODT, the streamwise velocity
254 must be positive everywhere on the line, so a small minimum velocity of
255 $v_{min} = 0.1 \text{ m}\cdot\text{s}^{-1}$ is specified and added across the entire velocity profile.

256 ODT simulations were performed with parameters $C = 5.25$, $\beta_{LES} = 3.5$,
257 and $Z = 400$. The value of Z is the same as the spatial simulations in [15],
258 and the values of C and β_{LES} were adjusted to give good agreement with
259 the experimental data. Note the close agreement of the C and Z parameters
260 here to the optimal values used for the pipe flow simulations ($C = 5$ and
261 $Z = 350$). This illustrates a level of robustness in the ODT parameters

and suggests that intermediate values could be successfully applied in both configurations.

1024 independent ODT realizations were performed and results were ensemble averaged. All quantities are normalized consistent with jet similarity scaling. Downstream locations are normalized by the jet diameter D , and radial locations are normalized by $(y - y_0)$, where y is the downstream location and $y_0 = 4D$ is the virtual origin used in [43].

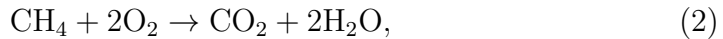
RESULTS AND PLOTS GO HERE

3.3. Jet Flame

ODT is uniquely suited for reacting flow simulations. Here, we present illustrative ODT simulation results of a round, turbulent jet flame based on and compared to the experimental DLR-A flame of Meier et al. [44]. This canonical flame configuration has been used extensively to study and validate turbulent combustion models [45, 46, 47, 48, 49, 50].

The DLR-A fuel stream is mixture of 22.1% CH_4 , 33.2% H_2 , and 44.7% N_2 (by volume) that issues into dry air via a nozzle with an inner diameter of 8 mm at a mean exit velocity of $42.2 \text{ m}\cdot\text{s}^{-1}$. The coflow air stream issues from a concentric nozzle 140 mm in diameter at a velocity of $0.3 \text{ m}\cdot\text{s}^{-1}$. The reported jet Reynolds number is 15,200.

Previous ODT studies of turbulent jet flames have used the temporal planar formulation, but the spatial cylindrical formulation developed recently [30] more closely matches the experimental configuration. This simulation uses the experimentally reported velocity profiles and jet dimensions. In the non-reacting case, a small minimum velocity was added uniformly to the velocity profile; no such addition is required here because of the slow-moving coflow air stream that issues alongside the reacting jet. The fuel was diluted with N_2 in the experimental flame to minimize radiative heat losses, and radiation is ignored in the simulation. This flame has a low Reynolds number, and the combustion chemistry proceeds quickly. The ODT simulation transports the chemical species O_2 , N_2 , CH_4 , H_2 , H_2O , and CO_2 . We assume that reactions proceed to the products of complete combustion and apply simple, fast reaction rates according to the following chemical equations:



These assumptions are not reasonable for the DLR-A flame, but they allow us to illustrate ODT in a reacting jet configuration with variable properties

283 and heat release, which is the primary purpose of this example case. More
284 complex combustion reaction mechanisms are available within the source
285 code and can be accessed by changing the appropriate input file parameter.

286 This simulation uses ODT parameters $C = 20$, $\beta_{LES} = 17$, and $Z = 400$.
287 The values of C and β_{LES} were adjusted to give good agreement with the
288 experimental data, and the value of Z is the same as it was for the non-
289 reacting jet in Section 3.2. 1024 independent flow realizations were performed
290 in parallel and the results ensemble averaged. Downstream distance y and
291 radial position r are normalized by the jet diameter D .

292 RESULTS AND PLOTS GO HERE

293 4. Impact

294 Questions to answer in this section (from SoftwareX template)

- 295 1. How can new research questions be pursued with this software?
 - 296 • possibility of parametric studies (much harder with DNS/LES/RANS)
 - 297 • study of late-flame soot and radiation interactions, soot emissions
298 as smoke
 - 299 • comparative radiation model studies?
- 300 2. How does the software improve pursuit of existing research questions?
 - 301 • late-flame behavior becomes easier to study
 - 302 • validation of LES subgrid models
 - 303 • soot stuff, especially late in the flame (because soot moves slowly
304 compared to gas species and therefore short simulation times like
305 in DNS aren't enough to study it effectively)
- 306 3. How does the software change the daily practice of its users?
 - 307 • cases take hours or days rather than weeks using supercomputer
308 resources
 - 309 • test cases can be run on local computers (unlike something like
310 DNS) and as background tasks without disrupting other tasks
 - 311 • ODT as a tool complements other approaches, can cover blind
312 spots and be used in validation
- 313 4. How widespread is the software? Who uses it? (Within and outside of
314 intended research area and/or group.)
 - 315 • BYU group
 - 316 • JCH at Sandia

- 317 • Chalmers group in Sweden (Marco Fistler, etc.)
- 318 • German university group (Heiko Schmidt, Juan Media, Marten
- 319 Klein, etc.)
- 320 • TO DO: find other groups who have used or currently use ODT
- 321 5. How is the software used in commercial settings (if any)? Has it led to
- 322 creation of spin-off companies?
- 323 • No commercial use (I think).

324 5. Conclusion

325 Write this part next to last

326 6. Conflict of Interest

327 We wish to confirm that there are no known conflicts of interest associated
 328 with this publication and there has been no significant financial support for
 329 this work that could have influenced its outcome.

330 Acknowledgements

331 This work was supported in part by the National Science Foundation
 332 under Grant No. CBET-1403403.

333 References

- 334 [1] D. O. Lignell, G. C. Fredline, A. D. Lewis, Comparison of one-
 335 dimensional turbulence and direct numerical simulations of soot for-
 336 mation and transport in a nonpremixed ethylene jet flame 35 (2) (2015)
 337 1199–1206. doi:10.1016/j.proci.2014.05.046.
- 338 [2] A. W. Abboud, C. Schulz, T. Saad, S. T. Smith, D. D. Harris, D. O.
 339 Lignell, A numerical comparison of precipitating turbulent flows between
 340 large-eddy simulation and one-dimensional turbulence 61 (10) (2015)
 341 3185–3197. doi:10.1002/aic.14870.
- 342 [3] A. R. Kerstein, One-dimensional turbulence: model formulation and ap-
 343 plication to homogeneous turbulence, shear flows, and buoyant stratified
 344 flows 392 (1999) 277–334. doi:10.1017/S0022112099005376.
- 345 [4] A. R. Kerstein, T. D. Dreeben, Prediction of turbulent free shear
 346 flow statistics using a simple stochastic model 12 (2) (2000) 418–424.
 347 doi:10.1063/1.870319.

- [5] A. R. Kerstein, W. T. Ashurst, S. Wunsch, V. Nilsen, One-dimensional turbulence: vector formulation and application to free shear flows 447 (2001) 85–109. doi:10.1017/S0022112001005778.
- [6] T. Echekki, A. R. Kerstein, T. D. Dreeben, J.-Y. Chen, ‘one-dimensional turbulence’ simulation of turbulent jet diffusion flames: model formulation and illustrative applications 125 (3) (2001) 1083–1105. doi:10.1016/S0010-2180(01)00228-0.
- [7] J. C. Hewson, A. R. Kerstein, Stochastic simulation of transport and chemical kinetics in turbulent $\text{co}/\text{h}_2/\text{n}_2$ flames 5 (4) (2001) 669–697. doi:10.1088/1364-7830/5/4/309.
- [8] J. C. Hewson, A. R. Kerstein, Local extinction and reignition in nonpremixed turbulent $\text{co}/\text{h}_2/\text{n}_2$ jet flames 174 (5-6) (2002) 35–66. doi:10.1080/713713031.
- [9] D. O. Lignell, D. S. Rappleye, One-dimensional-turbulence simulation of flame extinction and reignition in planar ethylene jet flames 159 (9) (2012) 2930–2943. doi:10.1016/j.combustflame.2012.03.018.
- [10] N. Punati, J. C. Sutherland, A. R. Kerstein, E. R. Hawkes, J. H. Chen, An evaluation of the one-dimensional turbulence model: Comparison with direct numerical simulations of co/h_2 jets with extinction and reignition 33 (1) (2011) 1515–1522. doi:10.1016/j.proci.2010.06.127.
- [11] A. Abdelsamie, D. O. Lignell, D. Thévenin, Comparison between odt and dns for ignition occurrence in turbulent premixed jet combustion: safety-relevant applications 231 (10) (2017) 1709–1735. doi:10.1515/zpch-2016-0902.
- [12] D. O. Lignell, V. B. Lansinger, A. R. Kerstein, A cylindrical formulation of the one-dimensional turbulence (odt) model for turbulent jet flames, in: AIChE Annual Meeting 2017, American Institute of Chemical Engineers, 2017.
- [13] B. Goshayeshi, J. C. Sutherland, Prediction of oxy-coal flame stand-off using high-fidelity thermochemical models and the one-dimensional turbulence model 35 (3) (2015) 2829–2837. doi:10.1016/j.proci.2014.07.003.
- [14] Z. Jozefik, A. R. Kerstein, H. Schmidt, S. Lyra, H. Kolla, J. H. Chen, One-dimensional turbulence modeling of a turbulent counterflow flame with comparison to dns 162 (8) (2015) 2999–3015. doi:10.1016/j.combustflame.2015.05.010.

- [15] E. I. Monson, D. O. Lignell, M. A. Finney, C. Werner, Z. Jozefik, A. R. Kerstein, R. S. Hintze, Simulation of ethylene wall fires using the spatially-evolving one-dimensional turbulence model 52 (1) (2016) 167–196. doi:10.1007/s10694-014-0441-2.
- [16] J. C. Hewson, A. J. Ricks, S. R. Tieszen, A. R. Kerstein, R. O. Fox, Conditional-moment closure with differential diffusion for soot evolution in fire, in: Center for Turbulence Research, Proceedings of the Summer Program 2006, Stanford University, 2006.
- [17] J. C. Hewson, A. J. Ricks, S. R. Tieszen, A. R. Kerstein, R. O. Fox, On the transport of soot relative to a flame: modeling differential diffusion for soot evolution in fire, in: H. Bockhorn, A. D’Anna, A. F. Sarofim, H. Wang (Eds.), Combustion Generated Fine Carbonaceous Particles, KIT Scientific Publishing, 2009, pp. 571–588.
- [18] D. O. Lignell, J. C. Hewson, One-dimensional turbulence simulation: overview and application to soot formation in nonpremixed flames, in: SIAM Conference on Computational Science and Engineering, 2015.
- [19] A. J. Ricks, J. C. Hewson, A. R. Kerstein, J. P. Gore, S. R. Tieszen, W. T. Ashurst, A spatially developing one-dimensional turbulence (odt) study of soot and enthalpy evolution in meter-scale buoyant turbulent flames 182 (1) (2010) 60–101. doi:10.1080/00102200903297003.
- [20] G. Sun, J. C. Hewson, D. O. Lignell, Evaluation of stochastic particle dispersion modeling in turbulent round jets 89 (2017) 108–122. doi:10.1016/j.ijmultiphaseflow.2016.10.005.
- [21] J. R. Schmidt, J. O. L. Wendt, A. R. Kerstein, Non-equilibrium wall deposition of inertial particles in turbulent flow 137 (2) (2009) 233–257. doi:10.1007/s10955-009-9844-8.
- [22] G. Sun, D. O. Lignell, J. C. Hewson, C. R. Gin, Particle dispersion in homogeneous turbulence using the one-dimensional turbulence model 26 (10) (2014) 103301. doi:10.1063/1.4896555.
- [23] M. Fistler, D. O. Lignell, A. R. Kerstein, M. Oevermann, Numerical studies of turbulent particle-laden jets using spatial approach of one-dimensional turbulence, in: ILASS-Europe 28th Conference on Liquid Atomization and Spray Systems, 2017.
- [24] S. Cao, T. Echehki, A low-dimensional stochastic closure model for combustion large-eddy simulation 9. doi:10.1080/14685240701790714.

- [25] R. C. Schmidt, A. R. Kerstein, S. Wunsch, V. Nilsen, Near-wall les closure based on one-dimensional turbulence modeling 186 (1) (2003) 317–355. doi:10.1016/S0021-9991(03)00071-8.
- [26] R. C. Schmidt, A. R. Kerstein, R. McDermott, Odtles: A multi-scale model for 3d turbulent flow based on one-dimensional turbulence modeling 199 (13-16) (2010) 865–880. doi:10.1016/j.cma.2008.05.028.
- [27] E. Gonzalez-Juez, A. R. Kerstein, D. O. Lignell, Fluxes across double-diffusive interfaces: a one-dimensional-turbulence study 677 (2011) 218–254. doi:10.1017/jfm.2011.78.
- [28] E. Gonzalez-Juez, A. R. Kerstein, D. O. Lignell, Reactive rayleigh–taylor turbulent mixing: a one-dimensional-turbulence study 107 (5) (2013) 506–525. doi:10.1080/03091929.2012.736504.
- [29] S. Wunsch, A. R. Kerstein, A model for layer formation in stably stratified turbulence 13 (3) (2001) 702–712. doi:10.1063/1.1344182.
- [30] D. O. Lignell, V. B. Lansinger, J. Medina, M. Klein, A. R. Kerstein, H. Schmidt, M. Fistler, M. Oevermann, One-dimensional turbulence modeling for cylindrical and spherical flows: model formulation and application 32 (4) (2018) 495–520. doi:10.1007/s00162-018-0465-1.
- [31] M. Klein, D. O. Lignell, H. Schmidt, Map-based modeling of turbulent convection: Application of the one-dimensional turbulence model to planar and spherical geometries, in: International Conference on Rayleigh-Benard Turbulence, 2018.
- [32] M. Klein, D. O. Lignell, H. Schmidt, Stochastic modeling of temperature and velocity statistics in spherical-shell convection, in: EGU Conference on Recent developments in Geophysical Fluid Dynamics, 2019.
- [33] W. T. Ashurst, A. R. Kerstein, One-dimensional turbulence: Variable-density formulation and application to mixing layers 17 (2). doi:10.1063/1.1847413.
- [34] D. O. Lignell, A. R. Kerstein, G. Sun, E. I. Monson, Mesh adaption for efficient multiscale implementation of one-dimensional turbulence 27 (3-4) (2013) 273–295. doi:10.1007/s00162-012-0267-9.
- [35] Y. A. Çengel, J. M. Cimbala, Fluid Mechanics, 2nd Edition, Çengel series in engineering thermal-fluid sciences, McGraw-Hill Higher Education, 2010.

- 452 [36] J. Beder, yaml-cpp v0.6.3 (2008).
 453 URL <https://github.com/jbeder/yaml-cpp/>
- 454 [37] A. C. Hindmarsh, R. Serban, D. R. Reynolds, CVODE,
 455 https://computing.llnl.gov/sites/default/files/public/cv_guide.pdf
 456 (2020).
 457 URL <https://computing.llnl.gov/projects/sundials/cvode>
- 458 [38] G. Strang, On the construction and comparison of difference schemes
 459 5 (3) (1968) 506–517. doi:10.1137/0705041.
- 460 [39] D. G. Goodwin, R. L. Speth, H. K. Moffat, B. W. Weber, Cantera
 461 (2018). doi:10.5281/zenodo.1174508.
 462 URL <https://cantera.org/>
- 463 [40] D. van Heesch, Doxygen (2018).
 464 URL <https://www.doxygen.nl/>
- 465 [41] G. K. El Khoury, P. Schlatter, A. Noorani, P. F. Fischer, G. Brethouwer,
 466 A. V. Johansson, Direct numerical simulation of turbulent pipe
 467 flow at moderately high reynolds numbers 91 (3) (2013) 475–495.
 468 doi:10.1007/s10494-013-9482-8.
- 469 [42] C. Chin, J. P. Monty, A. Ooi, Reynolds number effects in dns of pipe
 470 flow and comparison with channels and boundary layers 45 (2014) 33–40.
 471 doi:10.1016/j.ijheatfluidflow.2013.11.007.
- 472 [43] H. J. Hussein, S. P. Capp, W. K. George, Velocity measurements in a
 473 high-reynolds-number, momentum-conserving, axisymmetric, turbulent
 474 jet 258 (1994) 31–75. doi:10.1017/S002211209400323X.
- 475 [44] W. Meier, R. S. Barlow, Y.-L. Chen, J.-Y. Chen, Raman/Rayleigh/LIF
 476 measurements in a turbulent CH₄/H₂/N₂ jet diffusion flame: experi-
 477 mental techniques and turbulence–chemistry interaction 123 (3) (2000)
 478 326–343. doi:10.1016/S0010-2180(00)00171-1.
 479 URL <https://tnfworkshop.org/data-archives/simplejet/dlrflames/>
- 480 [45] H. Pitsch, Unsteady flamelet modeling of differential diffusion in tur-
 481 bulent jet diffusion flames 123 (3) (2000) 358–374. doi:10.1016/S0010-
 482 2180(00)00135-8.
- 483 [46] R. P. Lindstedt, H. Ozarovsky, Joint scalar transported pdf model-
 484 ing of nonpiloted turbulent diffusion flames 143 (4) (2005) 471–490.
 485 doi:10.1016/j.combustflame.2005.08.030.

- 486 [47] H. Wang, S. B. Pope, Large eddy simulation/probability density func-
 487 tion modeling of a turbulent $\text{CH}_4/\text{H}_2/\text{N}_2$ jet flame 33 (1) (2011) 1319–1330.
 488 doi:10.1016/j.proci.2010.08.004.
- 489 [48] M. Fairweather, R. M. Woolley, First-order conditional moment closure
 490 modeling of turbulent, nonpremixed methane flames 138 (1-2) (2004)
 491 3–19. doi:10.1016/j.combustflame.2004.03.001.
- 492 [49] K. W. Lee, D. H. Choi, Prediction of NO in turbulent diffusion
 493 flames using eulerian particle flamelet model 12 (5) (2008) 905–927.
 494 doi:10.1080/13647830802094351.
- 495 [50] K. W. Lee, D. H. Choi, Analysis of NO formation in high
 496 temperature diluted air combustion in a coaxial jet flame us-
 497 ing an unsteady flamelet model 52 (5-6) (2009) 1412–1420.
 498 doi:10.1016/j.ijheatmasstransfer.2008.08.015.

499 **Current executable software version**

500 Ancillary data table required for sub version of the executable software:
 501 (x.1, x.2 etc.) kindly replace examples in right column with the correct
 502 information about your executables, and leave the left column as it is.

Nr.	(Executable) software meta-data description	Please fill in this column
S1	Current software version	2.1
S2	Permanent link to executables of this version	For example: <i>https</i> : <i>//github.com/combogenomics/DuctApe/releases/tag/DuctApe - 0.16.4</i>
S3	Legal Software License	MIT
S4	Computing platforms/Operating Systems	Linux, OS X, Microsoft Windows
S5	Installation requirements & dependencies	CMake 3.12+, Cantera, Git, Doxygen (optional)
S6	If available, link to user manual - if formally published include a reference to the publication in the reference list	For example: <i>http</i> : <i>//mozart.github.io/documentation/</i>
S7	Support email for questions	davidlignell@byu.edu

Table 3: Software metadata (optional)